

"This is the peer reviewed version of the following article:

Christopher P. Barnett, Nathalie J. Nataren, Manuela Klingler-Hoffmann, Quenten Schwarz, Chan-Eng Chong, Young K. Lee, Damien L. Bruno, Jill Lipsett, Andrew J. McPhee, Andreas W. Schreiber, Jinghua Feng, Christopher N. Hahn, and Hamish S. Scott

Ectrodactyly and lethal pulmonary acinar dysplasia associated with homozygous FGFR2 mutations identified by exome sequencing

Human Mutation, 2016; 37(9):955-963

© 2016 Wiley Periodicals, Inc.

which has been published in final form at <http://dx.doi.org/10.1002/humu.23032>

This article may be used for non-commercial purposes in accordance with Wiley Terms and Conditions for Self-Archiving."

PERMISSIONS

<http://olabout.wiley.com/WileyCDA/Section/id-828039.html>

Publishing in a subscription based journal

Accepted (peer-reviewed) Version

The accepted version of an article is the version that incorporates all amendments made during the peer review process, but prior to the final published version (the Version of Record, which includes; copy and stylistic edits, online and print formatting, citation and other linking, deposit in abstracting and indexing services, and the addition of bibliographic and other material.

Self-archiving of the accepted version is subject to an embargo period of 12-24 months. The embargo period is 12 months for scientific, technical, and medical (STM) journals and 24 months for social science and humanities (SSH) journals following publication of the final article.

- the author's personal website
- the author's company/institutional repository or archive
- not for profit subject-based repositories such as PubMed Central

Articles may be deposited into repositories on acceptance, but access to the article is subject to the embargo period.

The version posted must include the following notice on the first page:

"This is the peer reviewed version of the following article: [FULL CITE], which has been published in final form at [Link to final article using the DOI]. This article may be used for non-commercial purposes in accordance with Wiley Terms and Conditions for Self-Archiving."

The version posted may not be updated or replaced with the final published version (the Version of Record). Authors may transmit, print and share copies of the accepted version with colleagues, provided that there is no systematic distribution, e.g. a posting on a listserve, network or automated delivery.

There is no obligation upon authors to remove preprints posted to not for profit preprint servers prior to submission.

7 September 2017

Research Article

Ectrodactyly and lethal pulmonary acinar dysplasia associated with homozygous *FGFR2* mutations identified by exome sequencing

Christopher P. Barnett^{1,4}, Nathalie J. Nataren^{2,3,4}, Manuela Klingler-Hoffmann^{2,3,4}, Quentin Schwarz³, Chan-Eng Chong², Young K. Lee², Damien L. Bruno⁶, Jill Lipsett⁷, Andrew J. McPhee^{5,8}, Andreas W. Schreiber^{3,4,9}, Jinghua Feng^{3,4,9}, Christopher N. Hahn^{2,3,5}, Hamish S. Scott^{2,3,4,5,9}

1) SA Clinical Genetics, Women's and Children's Hospital/SA Pathology, North Adelaide, SA, Australia;

2) Department of Genetics and Molecular Pathology, Centre for Cancer Biology, SA Pathology, Adelaide, SA, Australia;

3) Centre for Cancer Biology, An alliance between SA Pathology and the University of South Australia

4) School of Biological Sciences, University of Adelaide, SA, Australia;

5) School of Medicine, University of Adelaide, SA, Australia;

6) Cytogenetics Laboratory, Murdoch Children's Research Institute, Royal Children's Hospital, Parkville, Australia;

7) Department of Neonatal Medicine, Women's and Children's Hospital, North Adelaide, SA, Australia;

8) Department of Anatomical Pathology, Women's and Children's Hospital/SA Pathology, North Adelaide SA, Australia.

This article has been accepted for publication and undergone full peer review but has not been through the copyediting, typesetting, pagination and proofreading process, which may lead to differences between this version and the [Version of Record](#). Please cite this article as [doi: 10.1002/humu.23032](#).

This article is protected by copyright. All rights reserved.

9) *ACRF Cancer Genomics Facility, Centre for Cancer Biology, SA Pathology*

Grant Sponsor:

HSS is supported by an Australian National Health and Medical Research Council (NHMRC) fellowship (APP1023059).

Running Title: *FGFR2* mutation with ectrodactyly & acinar dysplasia

Word Count (20-30 pages): 20 pages (Words: 3615)

Number of Tables/Figures (max 6): 1 + 5

Abstract (max 200 words): 171

Colour Figures: 1 (Figure 4) (others can be B&W in print)

Supplementary Figures: 3

Corresponding Authors:

Prof Hamish S Scott

Department of Genetics and Molecular Pathology

Centre for Cancer Biology, An alliance between SA Pathology and the University of South

Australia

SA Pathology,

PO Box 14, Rundle Mall, SA, 5000

Ph: +618 8222 3651

Fax: +618 8222 3146

Email: hamish.scott@sa.gov.au

A/Professor Christopher Barnett MBBS FRACP FCCMG

Head, Paediatric and Reproductive Genetics

SA Clinical Genetics Service

Women's and Children's Hospital

72 King William Rd

North Adelaide 5006

South Australia

Ph: +618 8161 6279 or +618 8161 7375

Fax: +618 8161 7754

Email: christopher.barnett@sa.gov.au

ABSTRACT: Ectrodactyly/split hand-foot malformation is genetically heterogeneous with more than 100 syndromic associations. Acinar dysplasia is a rare congenital lung lesion of unknown etiology which is frequently lethal postnatally. To date, there have been no reports of combinations of these two phenotypes. Here we present an infant from a consanguineous union with both ectrodactyly and autopsy confirmed acinar dysplasia. SNP array and whole exome sequencing analyses of the affected infant identified a novel homozygous Fibroblast Growth Factor Receptor 2 (FGFR2) missense mutation (p.R255Q) in the IgIII domain (D3). Expression studies of *Fgfr2* in development show localization to the affected limbs and organs. Molecular modeling, and genetic and functional assays support that this mutation is at

least a partial loss-of-function mutation, and contributes to ectrodactyly and acinar dysplasia only in homozygosity, unlike previously reported heterozygous activating *FGFR2* mutations that cause Crouzon, Apert and Pfeiffer syndromes. This is the first report of mutations in a human disease with ectrodactyly with pulmonary acinar dysplasia and, as such, homozygous loss-of-function *FGFR2* mutations represent a unique syndrome.

Keywords: *FGFR2*, ectrodactyly, acinar dysplasia, whole exome sequencing

Introduction

Ectrodactyly/split-hand foot malformation (SHFM) can occur as an isolated abnormality but is also associated with more than 100 syndromes [Elliott and Evans 2006; Elliott et al., 2005]. At least 7 different genetic loci have been mapped [de Mollerat et al., 2003; Elliott and Evans 2006; Faiyaz-Ul-Haque et al., 2005; Goodman et al., 2002; Ianakiev et al., 2000; Naveed et al., 2006; Scherer et al., 1994; Ugur and Tolun 2008]. Acinar dysplasia (Congenital Pulmonary Airway Malformation (CPAM) type 0) is a rare perinatal lethal congenital lung disease [Chow et al., 2013; Lee 2013]. It is the rarest subtype of CPAM and is characterized embryologically by maturational arrest of the lung at the pseudo-glandular stage of development [Chow et al., 2013]. Familial cases of acinar dysplasia have been described and some reports describe associated congenital abnormalities. The etiology of acinar dysplasia is unknown [Lee 2013]. The combination of acinar dysplasia and ectrodactyly has not been described before.

Fibroblast growth factor receptor (FGFR2) (OMIM 176943) is a tyrosine kinase receptor and is one of four FGF receptors which have roles in the development and homeostasis of various tissues and the regulation of metabolism [Goetz and Mohammadi 2013]. When bound by a fibroblast growth factor (FGF), FGFR2 monomers dimerize resulting in transphosphorylation of tyrosine residues in the phosphotyrosine kinase domain. This activates the kinase activity of this receptor leading to the phosphorylation of intracellular targets [Goetz and Mohammadi 2013]. Fibroblast Receptor substrate 2 alpha (FRS2) (OMIM 607743), a target of FGFR2, lies immediately downstream of the receptor and mediates signaling through the MAP Kinase pathway [Gotoh et al., 2004; Gotoh et al., 2005]. ERK1/ERK2 (MAPK3/MAPK1, respectively), two components of this pathway, become phosphorylated when FGFR2 is activated and can traffic to the nucleus where they mediate effects of receptor activation. In the nucleus, they phosphorylate relevant targets, thereby promoting cellular proliferation and other events [Meister et al., 2013]. The ligand binding extracellular portion of FGFR2 is comprised of three immunoglobulin-like domains (D1, D2 and D3) [Goetz and Mohammadi 2013]. Alternative splicing of the C-terminal portion of the D3 domain determines ligand specificity. FGFR2 exists in two major isoforms (IIIb and IIIc), each of which has had the C-terminal end of the D3 domain encoded by a different exon. IIIb is expressed specifically in epithelial cells whilst IIIc is expressed in mesenchymal tissues [Eswarakumar et al., 2005]. FGFR2-associated disease is most often due to mutations in the IIIc isoform. Activating mutations in FGFR2 cause Crouzon syndrome (OMIM 123500) [Reardon et al., 1994], Apert syndrome (OMIM 101200) [Wilkie et al., 1995], Pfeiffer syndrome (OMIM 101600) [Muenke et al., 1994; Schell et al., 1995], Jackson-Weiss syndrome (OMIM 123150) [Jabs et al., 1994], Beare-Stevenson syndrome (OMIM 123790) [Przylepa et al., 1996], and non-syndromic craniosynostosis [Carinci et al., 2005; Reardon et al., 1994; Wilkie et al., 2007]. The majority of mutations in Crouzon syndrome occur in the D3 domain. Several of these

craniosynostosis syndromes have associated limb abnormalities (*e.g.* broad first finger/toe in Pfeiffer syndrome, syndactyly in Apert syndrome), but ectrodactyly is not a general feature of these conditions [Garcin et al., 1932] and no primary congenital pulmonary abnormalities have been previously described. However, studies in an *Fgfr2* mouse model that displays Apert syndrome-like phenotypic features showed defects in FGFR2 signaling resulting in defective mesenchymal differentiation, inhibition of terminal airway development and ultimately an “emphysema like” phenotype throughout the lungs [De Langhe et al., 2006].

Here we present a newborn infant of consanguineous parents with a proposed new syndrome of lethal acinar dysplasia and ectrodactyly in whom exome sequencing identified a homozygous *FGFR2* mutation (GRCh37/hg19; *Chr10:g.123,279,668C>T*; *NM_000141.4:c.764G>A*; *NP_000132.3:p.R255Q*; *FGFR2 IIIc*) (<http://www.lovd.nl/FGFR2>). The unique clinical presentation of acinar dysplasia and ectrodactyly and the absence of craniosynostosis in the affected infant, her heterozygous parents and her sibling, led to our hypothesis that the *FGFR2* mutation in this family is at least a partial loss-of-function mutation. We performed functional experiments to determine the effect of the p.R255Q mutation on the activity of *FGFR2* by measuring its effect on downstream signaling and to confirm whether *FGFR2* is expressed in the tissues involved in the phenotype of the affected infant. *In silico* modeling was also carried out to predict the impact of the p.R255Q mutation. This is the first instance of a homozygous *FGFR2* missense mutation causing disease in humans.

Materials and Methods

SNP Array Analysis

A SNP array (Illumina HumanCytoSNP-12 v2.1) was performed on the patient's genomic DNA from peripheral blood to identify copy number changes and regions of loss of heterozygosity due to consanguinity.

Whole Exome Sequencing (WES)

Whole exome capture (Agilent Whole Exome SureSelect V4 All Exon Capture Platform; Agilent Technologies, Mulgrave, Victoria Australia) and sequencing (Illumina HiSeq2000 platform; Illumina, Inc, San Diego, CA USA), targeting a total sequence of 51 MB were performed at the Australian Genome Research Facility (Parkville, Victoria). Samples were sequenced using a paired end 2 x100 sequencing protocol. Reads were mapped to hg19 and variants called and annotated as described previously [Gagliardi et al., 2014]. Variants from within regions of common descent were screened against dbSNP v135 and Exome Aggregation Consortium (ExAC, v0.3.1, <http://exac.broadinstitute.org>) databases. Filtering was carried out on the WES variants under the key assumptions that the disease is completely penetrant and that any variants present in the affected infant, which were also present in dbSNP v135 with a minor allele frequency (MAF) greater than 0.1%, were non-causative, and hence excluded. Homozygous variants within regions of loss of heterozygosity were preferentially considered to fit with the predicted autosomal recessive mode of inheritance. Variants then underwent SeattleSeq Annotation including Genomic Evolutionary Rate Profiling (GERP) [Cooper et al., 2005] and were screened using PolyPhen-2 and Combined Annotation Dependent Depletion (CADD, v1.3) [Kircher et al., 2014] to predict pathogenicity. Primers were designed to amplify regions containing top hit candidate SNVs from patient, parents and an unaffected sibling DNA, and Sanger sequencing was performed to confirm their presence and segregation.

Candidate Gene Expression Using *in situ* RNA Hybridization

The candidate genes were annotated with a locus specific database (Mouse Genome Informatics (MGI), Online Mendelian disease database (OMIM) and gene expression databases (GenePaint and BioGPS). Whole mount *in situ* RNA hybridizations were performed on the limbs of E11.5 and E12.5 embryonic C57BL/6 inbred mice according to a previously published method on the Intavis InsituPro VSi instrument in order to determine the expression pattern of *FGFR2* during digital development [Riddle et al., 1993]. These stages were chosen as development of the digits begins to take place during these times [Taher et al., 2011]. RNA *in situ* probes were designed to target the final exon junction in *FGFR2* (exon 17-18, 678 bp). The probe sequence was amplified from mouse genomic DNA with primers 5'CGAATTCTGACTCTCACAACCA'3 (FOR), 5'TAGGTGCATCAGGACATCCAT 3' (REV). Images were taken on a SZX10 stereo microscope (Olympus) mounted with a Micropublisher 3.3 digital camera (Q-Imaging). The images were processed with OpenLab 2.2 software.

Generation of FGFR2 WT and Mutant Expression Constructs

A pRcCMV plasmid expressing the mesenchymal isoform FGFR2 IIIc (*NM_000141.4*, NP_000132.3, transcript variant 1) (pRcCMV-FGFR2) was purchased from OriGene. Using site-directed mutagenesis, we generated pRcCMV-FGFR2(p.R255Q) and pRcCMV-FGFR2(C342Y) (a mutation causing constitutive receptor activation) and pRcCMV-Empty.

FGFR2 and ERK1/2 Phosphorylation Assays

Human Embryonic Kidney 293 (HEK293) cells were transfected with FGFR2 WT and mutant expression constructs using Lipofectamine 2000 (Life Technologies). The following day, after serum starvation, cells were stimulated with fibroblast growth factor 2 (FGF2) at 20 ng/ml for 5 and 15 min in the presence of 10 µg/ml heparin to promote high affinity FGF2 binding to FGFR2. Western blots were performed to assess the levels of FGFR2 tyrosine phosphorylation and downstream ERK1/2 phosphorylation (p-ERK1/2). Phosphorylation of

two tyrosine residues (Y653, Y654) in the activation loop of FGFR2 leads to activation of the receptor and downstream signaling [Eswarakumar et al., 2005]. Antibodies used: anti-phospho ERK1/2 rabbit monoclonal antibody (Cell Signalling Technology, #12638), anti-ERK1/2 rabbit monoclonal antibody (Cell Signalling Technology, #4695), anti-phosphotyrosine monoclonal antibody (Thermo Scientific, MA1-10443) and anti-BEK (C-17) (FGFR2) rabbit polyclonal antibody (Santa Cruz, sc-122).

Results

Clinical Details

The proband was born to healthy first cousin parents of Kurdish heritage; the mother was 20 years old and the father 23 years old. There was no history of infertility or miscarriages. First-trimester nuchal translucency and biochemical screening were normal. Ultrasound examination at 19 weeks gestation revealed abnormalities of the hands and feet. On the left hand the thumb, second, third and fourth fingers were short and the fifth was thought to be absent. On the right hand only the index finger was seen. The arm bones appeared to be normal on both sides. On both feet, only the first and fifth toe could be identified. In addition to the limb abnormalities, there was evidence of echogenicity of the fetal gut. Parental hemoglobin electrophoresis and alpha thalassemia genotyping were normal. The couple was counselled regarding the differential diagnosis for these abnormalities, declined amniocentesis and elected to continue the pregnancy. The female infant was born at 36 weeks gestation following spontaneous onset of labour. Birthweight was 2.3 kg (15th percentile). The infant was in poor condition at birth (Apgar 2¹⁴⁵) and required immediate ventilatory support for severe respiratory distress. Chest x-ray was consistent with severe pulmonary hypoplasia and ventilatory support was withdrawn at 5 hours of age; the infant died shortly

after. Dysmorphic facial features were noted with epicanthic folds, a small mouth (23 mm, normal range 26 ± 2.5 mm), mild hypertelorism (78 mm, normal range 65 ± 3.5 mm), a broad nasal bridge and bulbous nasal tip, low set ears and obvious narrowing of the external auditory canals bilaterally which remained patent (Figure 1A and B). The fontanelles were normal and there were no features to suggest craniosynostosis. Both parents had normal physical examinations. X-ray of the mother's skull showed no abnormalities (Supp. Figure S1).

There were 4 digits on the left hand and a cleft extending into the palm between fingers 2 and 3 (Figure 1C, D and H). There was skin syndactyly between fingers 1 and 2, and fingers 3 and 4. Fingers 1-3 were considerably shorter than the fourth finger. There was no recognizable thumb. Only one digit was recognizable on the right hand and this digit was attached to a broad base (Figure 1E and 1J). There were 4 digits identifiable on the right foot with the appearance of a bifid first toe and a cleft extending into the dorsum of the right foot between the bifid first/second toe and toes 4 and 5 (Figure 1F). There were 4 recognizable digits on the left foot including a large first toe (not shown). There was syndactyly between the second and third toes on this foot and a cleft between the first and second toes. These limb abnormalities were thought to represent a severe form of ectrodactyly with both oligodactyly and syndactyly. X-rays of the hands (Figure 1G corresponding to Figure 1H, and Figure 1I corresponding to Figure 1J) and feet performed at autopsy confirmed a disorganized pattern with absent or short phalanges, variable degrees of syndactyly, ectrodactyly, oligodactyly and bifid bones. Skeletal radiological survey was otherwise normal with no abnormalities of the cranial vault. The lungs were small at autopsy (combined weight 26.89 g; normal for 36 week female 36.7 ± 16.8 g) and had abnormal lobation with 2 lobes on the right and one on the left (Figure 1K). Histological examination demonstrated severe

maturational arrest of lung tissue at the pseudoglandular stage and multiple small cysts of <0.5 cm in diameter consistent with a diagnosis of acinar dysplasia (Figure 1L and 1M).

SNP Array and Whole Exome Sequencing to Identify Causal Candidate Gene Mutations

No significant copy number changes were identified in the genome of the affected infant using SNP array. There were however long continuous stretches of homozygosity representing approximately 6% of the genome, consistent with the degree of consanguinity expected for offspring of first cousins.

Whole exome sequencing (WES) was then performed on the affected infant, and following removal of variants present at a MAF>0.1% in dbSNP v135, coding variants were identified in 21 genes within the regions of loss of heterozygosity (LOH). These were further filtered to remove unlikely pathogenic variants with PolyPhen2 (benign), GERP (<2) and CADD (<10) using SeattleSeq Annotation which further narrowed down the number to 13 candidate variants. Analysis of gene expression patterns matching sites of developmental perturbations in the infant with The e-Mouse Atlas Project and Mouse Genome Informatics resulted in 5 genes; *FGFR2*, *GGA3*, *COL12A1*, *UBE2Q2* and *SPATA13*. Segregation analysis of the 5 variants on both parents, the affected infant and her sibling using Sanger sequencing was consistent with autosomal recessive inheritance of the disease for all variants except for *SPATA13* which was homozygous in the unaffected sibling and hence was excluded.

Of the 4 remaining genes, the mutation in *FGFR2* (p.R255Q; Table 1) was considered to be the most likely causative gene based on Online Mendelian Inheritance in Man (OMIM) phenotypes, expression data (BioGPS), a *FGFR2* mouse model [Mai et al., 2010], *in silico* modeling, and functional studies (outlined below). Sanger sequencing of each family member for segregation of *FGFR2* (p.R255Q) is shown in Figure 2A and B. Variants in *GGA3*,

COL12A1 and *UBE2Q2* were excluded as candidates due to clinical, phenotypic and/or expression inconsistencies when compared to the affected individual (Table 1).

FGFR2 Expression Marks Tissues Affected in this Patient

To more clearly define the expression profile of *FGFR2* in developing limbs and lungs, we performed *in situ* RNA hybridization on a staged series of mouse embryos. *FGFR2* expression was seen in the developing limbs at day E11.5 and E12.5. At E11.5, there was strong expression in the hindlimbs and forelimbs, specifically in mesenchymal condensations that will later give rise to bone (Figure 3A). By E12.5, *FGFR2* expression was localized to the webbing between the developing digits in the forelimbs and hindlimbs, tissues consistent with the aberrant development seen in the patient. Expression was also seen in the developing epithelium of E14.5 lungs which is consistent with the defects associated with acinar dysplasia (Figure 3B).

An Important Role for R255 in the Protein – *in silico* Modeling

The wildtype R255 amino acid residue in *FGFR2* and its surrounding sequence is highly conserved across multiple species including chimpanzee, mouse, chicken and zebrafish, and in all human *FGFR* family members (Figure 4A and Supp. Figure S2). The p.R255Q variant is situated at the D3 domain end of the linker between domains D2 and D3 (Figure 4B), and within a hotspot of germline mutations that cause Crouzon and Apert syndromes and non-syndromic craniosynostosis (Figure 4C). R255 with H254 and I348 forms a pocket for the binding of a sulfate ion from heparan sulphate (Figure 4D, top), [Golovin et al., 2005; Stauber et al., 2000] a glycoprotein that facilitates high affinity binding of the FGF ligand to the *FGFR2* receptor [Plotnikov et al., 2000] which is a necessary for active signaling from the cytoplasmic receptor tyrosine kinase [Stauber et al., 2000]. The p.R255Q mutation likely

prevents binding of this sulfate ion, which may impact on receptor activation and downstream signaling (Figure 4D, bottom).

FGFR2 (p.R255Q) Displays Loss-Of-Function Properties

To ascertain the functional effect of the p.R255Q mutation on FGFR2 signaling, we measured phosphorylation of FGFR2 and its downstream effectors ERK1/2 in response to the activating ligand FGF2. Phosphorylation of 2 tyrosine residues (Y653 and Y654) in the activation loop of FGFR2 leads to activation and signaling of the receptor [Eswarakumar et al., 2005]. As a positive control, we included a known Crouzon syndrome mutation C342Y, which causes homodimerization and constitutive activation of FGFR2 resulting in increased basal ERK1/2 phosphorylation [Krejci et al., 2012]. Human Embryonic Kidney 293 (HEK293) cells were transiently transfected with constructs to express FGFR2 WT and mutants. Following a period of serum starvation, the cells were stimulated with FGF2 for 5 and 15 min. FGFR2 (p.R255Q) mutant displayed similar basal receptor phosphorylation as WT, but in response to FGF2, did not achieve the same level of increased FGFR2 phosphorylation, which is seen more notably in downstream ERK1/2 phosphorylation, as did WT (Figure 5 and Supp. Figure S3). For FGFR2 phosphorylation, 4 individual blots are shown as they were difficult to quantify due to the large size of the protein and spread of the bands. C342Y showed high basal FGFR2 phosphorylation and heightened basal and FGF2-stimulated ERK1/2 activation consistent with a constitutively active mutant. Overall, p.R255Q demonstrates properties of at least a partial loss-of-function mutation consistent with its recessive inheritance pattern.

Discussion

This case of a unique phenotype of ectrodactyly and acinar dysplasia represents the first human case of homozygous *FGFR2* disease to the best of our knowledge. RNA *in situ* hybridization data revealed expression in the affected tissues in mice (forelimbs, hindlimbs and the lung) and protein alignments revealed a high level of conservation for the R255 residue. *Fgfr2* knockout mice show complete absence of limb outgrowth and defects in lung branching morphogenesis [Arman et al., 1999]. Further, a homozygous knock-in mouse model of a gain-of-function *Fgfr2*^{W290R} mutant developed by others overlaps most of the abnormalities observed in our patient [Mai et al., 2010]. Interestingly however, while *Fgfr2*^{W290R/+} mice have normal limb development consistent with Crouzon syndrome, *Fgfr2*^{W290R/W290R} developed major reductive limb abnormalities and small lungs and died on the first day of life. It is clear that the lungs in this mouse model are markedly small and underdeveloped [Mai et al., 2010]. The *Fgfr2*^{W290R/W290R} mice also displayed abnormalities of the cranial vault, although no craniosynostosis was seen consistent with observations for our infant with homozygous *FGFR2*^{R255Q/R255Q} mutation. The overall analysis of *FGFR2* gain-of-function and loss-of-function mouse models suggest that various organs respond differently to heterozygous and homozygous mutant genotypes. Further, in some tissues, perturbation of *FGFR2* signaling, either up or down, results in the same phenotype while in other tissues produces opposite effects (summarized in Mai et al., [2010]). The predominantly distal pattern of limb abnormalities in our case may suggest more complex involvement of *FGFR2* in human limb development or result from this at least partial loss-of-function mutation.

Consistent with loss-of-function of *FGFR2* in our patient causing lung and limb abnormalities is phenotypic data from a mouse model of homozygous loss-of-function mutation in *FGF10*, an endogenous ligand of *FGFR2* [Sekine et al., 1999]. In this study, homozygous *FGF10*-deficient mice died at birth due to lack of lung development. Severe pulmonary branching morphology was disrupted. Mutant mice also had complete truncation of the fore- and

hindlimbs [Sekine et al., 1999]. Based on genetic inheritance pattern, functional studies, and our patient and parental phenotypes, we propose that the homozygous FGFR2 mutation is most likely a loss-of-function. FGF2 stimulation assays showed that this mutation displays decreased but not completely abrogated activation and signaling in downstream pathways, providing evidence of at least partial loss-of-function. Furthermore, segregation analysis supports the candidacy of this gene and *in situ* RNA hybridization in mice point to the involvement of this gene in limb and lung development. Further functional work will be required to confirm the exact mechanism by which this gene mutation leads to loss-of-function of FGFR2.

Gain-of-function mutations in FGFR2 have consistently caused craniosynostosis syndromes [Hatch et al., 2006]. These gain-of-function mutations in craniosynostosis syndromes are thought to do so through receptor activation and some are glycosylation-dependent [Hatch et al., 2006]. In our study, we provide evidence that the FGFR2 p.R255Q mutation is at least partial loss-of-function. Neither parent has evidence of craniosynostosis on physical examination; the mother has had a skull x-ray with no evidence of craniosynostosis and both the father and the heterozygous sibling have no evidence of craniosynostosis. Similarly, dominant activating mutations in FGFR3 cause a variety of short-limbed bone dysplasias including achondroplasia and syndromic craniosynostosis. But recently, WES identified a homozygous loss-of-function mutation in FGFR3 in humans characterized by tall stature and severe skeletal abnormalities leading to inability to walk, with camptodactyly, arachnodactyly, and scoliosis [Makrythanasis et al., 2014].

Somatic loss-of-function mutations in FGFR2 are associated with malignant melanoma, but no previous cases of germline FGFR2 loss-of-function mutations have been described [Gartside et al., 2009]. The combination of acinar dysplasia with ectrodactyly has not been previously reported although there is one report of ectrodactyly and capillary alveolar

dysplasia, another lethal lung disease, in association with tibial agenesis [Witters et al., 2001]. Three children in one consanguineous family were affected, suggestive of autosomal recessive inheritance. The first infant died in the neonatal period of pulmonary hypertension, secondary to congenital alveolar capillary dysplasia and had tibial agenesis and ectrodactyly. The second infant had similarly severely affected lungs but normal limbs. A third affected pregnancy occurred with bilateral agenesis of the tibia, symmetric ectrodactyly of the hands and feet and alveolar capillary dysplasia. The genetic cause of these familial abnormalities has not been identified (personal communication with Witters). Isolated alveolar capillary dysplasia with misalignment of pulmonary veins (ACDMPV; OMIM 265380) is caused by heterozygous mutations in *FOXF1* (OMIM 601089) or its regulatory region and follows an autosomal dominant mode of inheritance [Sen et al., 2013]. *FOXF1* is expressed in developing capillaries rather than developing epithelium. It is interesting that germline mutations in Crouzon syndrome and somatic mutations in endometrial cancer have been shown to be gain-of-function while somatic mutations in melanoma are loss-of-function [Gartside et al., 2009]. For these three conditions, there are no mutations in common although they are somewhat scattered linearly along the primary protein sequence. Hence, for any newly identified variant, it may be very difficult to predict its phenotypic impact without functional testing.

Here we report a novel germline *FGFR2* mutation which displays yet another phenotype, and which is flanked immediately by Crouzon syndrome mutations. In our unique case, we have identified a homozygous at least partial loss-of-function mutation in *FGFR2* associated with a severe phenotype including lethal lung disease and marked limb abnormalities.

Acknowledgments

We would like to thank the family for participating in this study.

Disclosure statement: The authors declare that no conflict of interest exists.

Contributors

CPB, JL and AJM performed clinical diagnoses and analysis. DLB, AWS and JF performed SNP array, WES and bioinformatics analysis. NJN, MKH, QS, CEC and YL performed expression and functional studies. JF performed protein structure modeling. CPB, CNH and HSS completed overall data analysis and interpretation, and wrote the manuscript. All coauthors have approved the final version of the manuscript.

References

- Arman E, Haffner-Krausz R, Gorivodsky M, Lonai P. 1999. Fgfr2 is required for limb outgrowth and lung-branching morphogenesis. *Proc Natl Acad Sci U S A* 96(21):11895-9.
- Carinci F, Pezzetti F, Locci P, Becchetti E, Carls F, Avantaggiato A, Becchetti A, Carinci P, Baroni T, Bodo M. 2005. Apert and Crouzon syndromes: clinical findings, genes and extracellular matrix. *J Craniofac Surg* 16(3):361-8.
- Chow CW, Massie J, Ng J, Mills J, Baker M. 2013. Acinar dysplasia of the lungs: variation in the extent of involvement and clinical features. *Pathology* 45(1):38-43.
- Cooper GM, Stone EA, Asimenos G, Green ED, Batzoglou S, Sidow A. 2005. Distribution and intensity of constraint in mammalian genomic sequence. *Genome Res* 15(7):901-13.

- De Langhe SP, Carraro G, Warburton D, Hajihosseini MK, Bellusci S. 2006. Levels of mesenchymal FGFR2 signaling modulate smooth muscle progenitor cell commitment in the lung. *Dev Biol* 299(1):52-62.
- de Mollerat XJ, Gurrieri F, Morgan CT, Sangiorgi E, Everman DB, Gaspari P, Amiel J, Bamshad MJ, Lyle R, Blouin JL, Allanson JE, Le Marec B, et al. 2003. A genomic rearrangement resulting in a tandem duplication is associated with split hand-split foot malformation 3 (SHFM3) at 10q24. *Hum Mol Genet* 12(16):1959-71.
- Elliott AM, Evans JA. 2006. Genotype-phenotype correlations in mapped split hand foot malformation (SHFM) patients. *Am J Med Genet A* 140(13):1419-27.
- Elliott AM, Evans JA, Chudley AE. 2005. Split hand foot malformation (SHFM). *Clin Genet* 68(6):501-5.
- Eswarakumar VP, Lax I, Schlessinger J. 2005. Cellular signaling by fibroblast growth factor receptors. *Cytokine Growth Factor Rev* 16(2):139-49.
- Faiyaz-Ul-Haque M, Zaidi SH, King LM, Haque S, Patel M, Ahmad M, Siddique T, Ahmad W, Tsui LC, Cohn DH. 2005. Fine mapping of the X-linked split-hand/split-foot malformation (SHFM2) locus to a 5.1-Mb region on Xq26.3 and analysis of candidate genes. *Clin Genet* 67(1):93-7.
- Gagliardi L, Schreiber AW, Hahn CN, Feng J, Cranston T, Boon H, Hotu C, Oftedal BE, Cutfield R, Adelson DL, Braund WJ, Gordon RD, et al. 2014. ARMC5 mutations are common in familial bilateral macronodular adrenal hyperplasia. *J Clin Endocrinol Metab* 99(9):E1784-92.
- Garcin M, Thurel R, Rudaux P. 1932. Sur un cas isole de dysostose craniofaciale (maladie de Crouzon) avec ectrodactylie. *Bull Soc Med Hop Paris* 56:1458-1466.
- Gartside MG, Chen H, Ibrahim OA, Byron SA, Curtis AV, Wellens CL, Bengston A, Yudit LM, Eliseenkova AV, Ma J, Curtin JA, Hyder P, et al. 2009. Loss-of-function

- fibroblast growth factor receptor-2 mutations in melanoma. *Mol Cancer Res* 7(1):41-54.
- Goetz R, Mohammadi M. 2013. Exploring mechanisms of FGF signalling through the lens of structural biology. *Nat Rev Mol Cell Biol* 14(3):166-80.
- Golovin A, Dimitropoulos D, Oldfield T, Rachedi A, Henrick K. 2005. MSDsite: a database search and retrieval system for the analysis and viewing of bound ligands and active sites. *Proteins* 58(1):190-9.
- Goodman FR, Majewski F, Collins AL, Scambler PJ. 2002. A 117-kb microdeletion removing HOXD9-HOXD13 and EVX2 causes synpolydactyly. *Am J Hum Genet* 70(2):547-55.
- Gotoh N, Laks S, Nakashima M, Lax I, Schlessinger J. 2004. FRS2 family docking proteins with overlapping roles in activation of MAP kinase have distinct spatial-temporal patterns of expression of their transcripts. *FEBS Lett* 564(1-2):14-8.
- Gotoh N, Manova K, Tanaka S, Murohashi M, Hadari Y, Lee A, Hamada Y, Hiroe T, Ito M, Kurihara T, Nakazato H, Shibuya M, et al. 2005. The docking protein FRS2alpha is an essential component of multiple fibroblast growth factor responses during early mouse development. *Mol Cell Biol* 25(10):4105-16.
- Hatch NE, Hudson M, Seto ML, Cunningham ML, Bothwell M. 2006. Intracellular retention, degradation, and signaling of glycosylation-deficient FGFR2 and craniosynostosis syndrome-associated FGFR2C278F. *J Biol Chem* 281(37):27292-305.
- Ianakev P, Kilpatrick MW, Toudjarska I, Basel D, Beighton P, Tsipouras P. 2000. Split-hand/split-foot malformation is caused by mutations in the p63 gene on 3q27. *Am J Hum Genet* 67(1):59-66.

- Jabs EW, Li X, Scott AF, Meyers G, Chen W, Eccles M, Mao JI, Charnas LR, Jackson CE, Jaye M. 1994. Jackson-Weiss and Crouzon syndromes are allelic with mutations in fibroblast growth factor receptor 2. *Nat Genet* 8(3):275-9.
- Kircher M, Witten DM, Jain P, O'Roak BJ, Cooper GM, Shendure J. 2014. A general framework for estimating the relative pathogenicity of human genetic variants. *Nat Genet* 46(3):310-5.
- Krejci P, Aklian A, Kaucka M, Sevcikova E, Prochazkova J, Masek JK, Mikolka P, Pospisilova T, Spoustova T, Weis M, Paznekas WA, Wolf JH, et al. 2012. Receptor tyrosine kinases activate canonical WNT/beta-catenin signaling via MAP kinase/LRP6 pathway and direct beta-catenin phosphorylation. *PLoS One* 7(4):e35826.
- Lee EY. 2013. Interstitial lung disease in infants: new classification system, imaging technique, clinical presentation and imaging findings. *Pediatr Radiol* 43(1):3-13; quiz p 128-9.
- Mai S, Wei K, Flenniken A, Adamson SL, Rossant J, Aubin JE, Gong SG. 2010. The missense mutation W290R in *Fgfr2* causes developmental defects from aberrant IIIb and IIIc signaling. *Dev Dyn* 239(6):1888-900.
- Makrythanasis P, Temtamy S, Aglan MS, Otaify GA, Hamamy H, Antonarakis SE. 2014. A novel homozygous mutation in *FGFR3* causes tall stature, severe lateral tibial deviation, scoliosis, hearing impairment, camptodactyly, and arachnodactyly. *Hum Mutat* 35(8):959-63.
- Meister M, Tomasovic A, Banning A, Tikkanen R. 2013. Mitogen-Activated Protein (MAP) Kinase Scaffolding Proteins: A Recount. *Int J Mol Sci* 14(3):4854-84.

- Muenke M, Schell U, Hehr A, Robin NH, Losken HW, Schinzel A, Pulleyn LJ, Rutland P, Reardon W, Malcolm S, Winter RM. 1994. A common mutation in the fibroblast growth factor receptor 1 gene in Pfeiffer syndrome. *Nat Genet* 8(3):269-74.
- Naveed M, Al-Ali MT, Murthy SK, Al-Hajali S, Al-Khaja N, Deutsch S, Bottani A, Antonarakis SE, Nath SK, Radhakrishna U. 2006. Ectrodactyly with aplasia of long bones (OMIM; 119100) in a large inbred Arab family with an apparent autosomal dominant inheritance and reduced penetrance: clinical and genetic analysis. *Am J Med Genet A* 140(13):1440-6.
- Plotnikov AN, Hubbard SR, Schlessinger J, Mohammadi M. 2000. Crystal structures of two FGF-FGFR complexes reveal the determinants of ligand-receptor specificity. *Cell* 101(4):413-24.
- Przylepa KA, Paznekas W, Zhang M, Golabi M, Bias W, Bamshad MJ, Carey JC, Hall BD, Stevenson R, Orlow S, Cohen MM, Jr., Jabs EW. 1996. Fibroblast growth factor receptor 2 mutations in Beare-Stevenson cutis gyrate syndrome. *Nat Genet* 13(4):492-4.
- Reardon W, Winter RM, Rutland P, Pulleyn LJ, Jones BM, Malcolm S. 1994. Mutations in the fibroblast growth factor receptor 2 gene cause Crouzon syndrome. *Nat Genet* 8(1):98-103.
- Riddle RD, Johnson RL, Laufer E, Tabin C. 1993. Sonic hedgehog mediates the polarizing activity of the ZPA. *Cell* 75(7):1401-16.
- Schell U, Hehr A, Feldman GJ, Robin NH, Zackai EH, de Die-Smulders C, Viskochil DH, Stewart JM, Wolff G, Ohashi H, Price RA, Cohen MM, et al. 1995. Mutations in FGFR1 and FGFR2 cause familial and sporadic Pfeiffer syndrome. *Hum Mol Genet* 4(3):323-8.

- Scherer SW, Poorkaj P, Allen T, Kim J, Geshuri D, Nunes M, Soder S, Stephens K, Pagon RA, Patton MA, Berg MA, Donlon T, et al. 1994. Fine mapping of the autosomal dominant split hand/split foot locus on chromosome 7, band q21.3-q22.1. *Am J Hum Genet* 55(1):12-20.
- Sekine K, Ohuchi H, Fujiwara M, Yamasaki M, Yoshizawa T, Sato T, Yagishita N, Matsui D, Koga Y, Itoh N, Kato S. 1999. Fgf10 is essential for limb and lung formation. *Nat Genet* 21(1):138-41.
- Sen P, Yang Y, Navarro C, Silva I, Szafranski P, Kolodziejska KE, Dharmadhikari AV, Mostafa H, Kozakewich H, Kearney D, Cahill JB, Whitt M, et al. 2013. Novel FOXF1 mutations in sporadic and familial cases of alveolar capillary dysplasia with misaligned pulmonary veins imply a role for its DNA binding domain. *Hum Mutat* 34(6):801-11.
- Stauber DJ, DiGabriele AD, Hendrickson WA. 2000. Structural interactions of fibroblast growth factor receptor with its ligands. *Proc Natl Acad Sci U S A* 97(1):49-54.
- Taher L, Collette NM, Muruges D, Maxwell E, Ovcharenko I, Loots GG. 2011. Global gene expression analysis of murine limb development. *PLoS One* 6(12):e28358.
- Ugur SA, Tolun A. 2008. Homozygous WNT10b mutation and complex inheritance in Split-Hand/Foot Malformation. *Hum Mol Genet* 17(17):2644-53.
- Wilkie AO, Bochukova EG, Hansen RM, Taylor IB, Rannan-Eliya SV, Byren JC, Wall SA, Ramos L, Venancio M, Hurst JA, O'Rourke A W, Williams LJ, et al. 2007. Clinical dividends from the molecular genetic diagnosis of craniosynostosis. *Am J Med Genet A* 143A(16):1941-9.
- Wilkie AO, Slaney SF, Oldridge M, Poole MD, Ashworth GJ, Hockley AD, Hayward RD, David DJ, Pulleyn LJ, Rutland P, Malcolm S, Winter RM, et al. 1995. Apert

syndrome results from localized mutations of FGFR2 and is allelic with Crouzon syndrome. *Nat Genet* 9(2):165-72.

Witters I, Devriendt K, Moerman P, Caudron J, Van Hole C, Fryns JP. 2001. Bilateral tibial agenesis with ectrodactyly (OMIM 119100): further evidence for autosomal recessive inheritance. *Am J Med Genet* 104(3):209-13.

Figure Legends

Figure 1. Anatomical and histological features of affected infant. **A** and **B**: Head and face, **C** and **D**: left hand, and **E**: right hand. X-rays of **G** and **H**: left hand and **I** and **J**: right hand. Acinar dysplasia of affected infant's autopsy lung at 36 weeks gestation. **K**: Photograph of heart and lungs showing greatly reduced lung size. Hematoxylin and Eosin staining of **L**: affected infant's lung showing acinar dysplasia in comparison to **M**: normal lung of a similar aged individual.



Figure 2. Pedigree of infant affected with ectrodactyly and acinar dysplasia and segregation analysis of *FGFR2* (p.R255Q) mutation. **A:** Pedigree of affected family showing *FGFR2* genotype. **B:** Sanger sequencing of *FGFR2* mutation in affected family confirms parental heterozygosity and affected infant homozygosity for *NM_000141.4:c.764G>A* (NP_000132.3:p.R255Q).

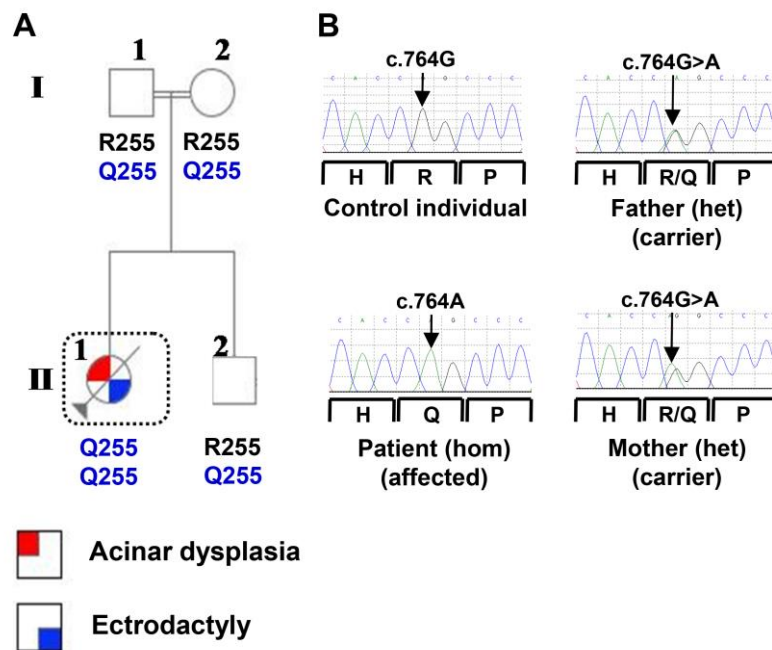


Figure 3. *FGFR2* *in situ* RNA hybridization of embryonic mouse. **A:** Whole mount *in situ* of mouse embryo limbs at embryonic day 11.5 and 12.5. **B:** Sagittal section of *in situ* RNA hybridization of embryonic mouse E14.5 (Image from genepaint.org, image set ID:FG35, Image 5D).

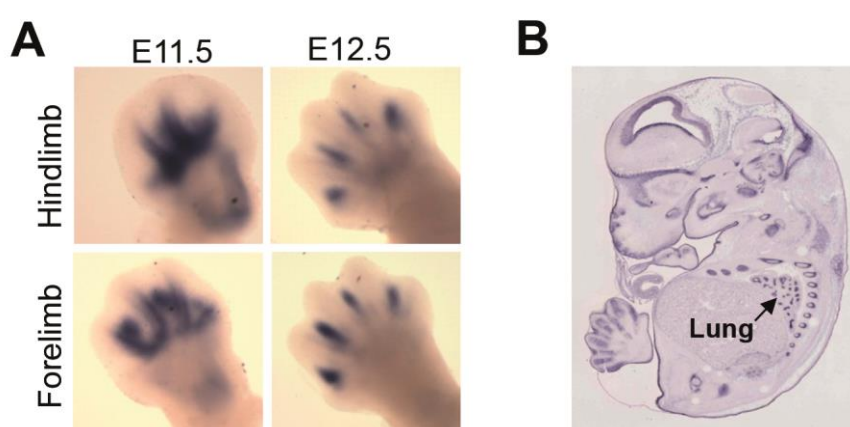


Figure 4. Conservation of *FGFR2* R255 across species and structural modeling to show its function. **A:** Conservation of amino acid R255 in *FGFR2* across species. Multiple Alignment in HomoloGene (NCBI) was used to align the orthologous amino acid residues to human R255 and surrounding sequence in the species shown. Extracellular immunoglobulin-like domains D2 and D3 are shown below alignments. **B:** Position of known *FGFR2* disease-causing mutations and R255Q. R255Q (orange) is located in the D3 Ig-like domain of *FGFR2* near the ligand binding surface. Previously identified activating mutations from HGMD® Human Gene Mutation Database (BIOBASE) (green) are predominantly located throughout the D3 domain. **C:** Position of R255Q in the *FGFR2* protein in relation to other disease-causing activating mutations. Shown is *FGFR2* (NM_000141.4, variant 1; NP_000132.3, isoform IIIc) with immunoglobulin-like domains (D1-3, bind FGF ligands),

acidic box (AB, binds bivalent cations for optimal interaction with heparin sulfate proteoglycans), transmembrane domain (TM) and tyrosine kinase domain (kinase). Crouzon (orange), Pfeiffer (purple) and Apert (green) syndromes, non-syndromic craniosynostosis and others (blue). Mutations were obtained from Human Gene Mutation Database (HGMD). **D:** Effect of p.R255Q on FGFR2 binding to its ligand. Molecular structure of human FGF1 ligand (pale yellow) to wild-type (WT) human FGFR2 (D3 in deep blue and D2 in light blue). Negatively charged sulphate ions (green) from ligand-associated heparin sulphate are able to associate with the WT R255 (orange) and adjacent residues H254 (pink) and I348 (magenta). R255Q leads to the replacement of a large, positive side chain with a smaller neutral one, which may negatively impact binding of heparin sulphate to the receptor, leading to a loss of receptor activation. The loss of this charged chain is also predicted to alter the confirmation of the D3 Ig-like domain which may further inhibit activation. The WT crystal structure (PDB ID: 1DJS) is from Stauber *et al.* [Stauber et al., 2000]. Visualization is via PyMOL (Version 1.5.0.3 Schrödinger, LLC).

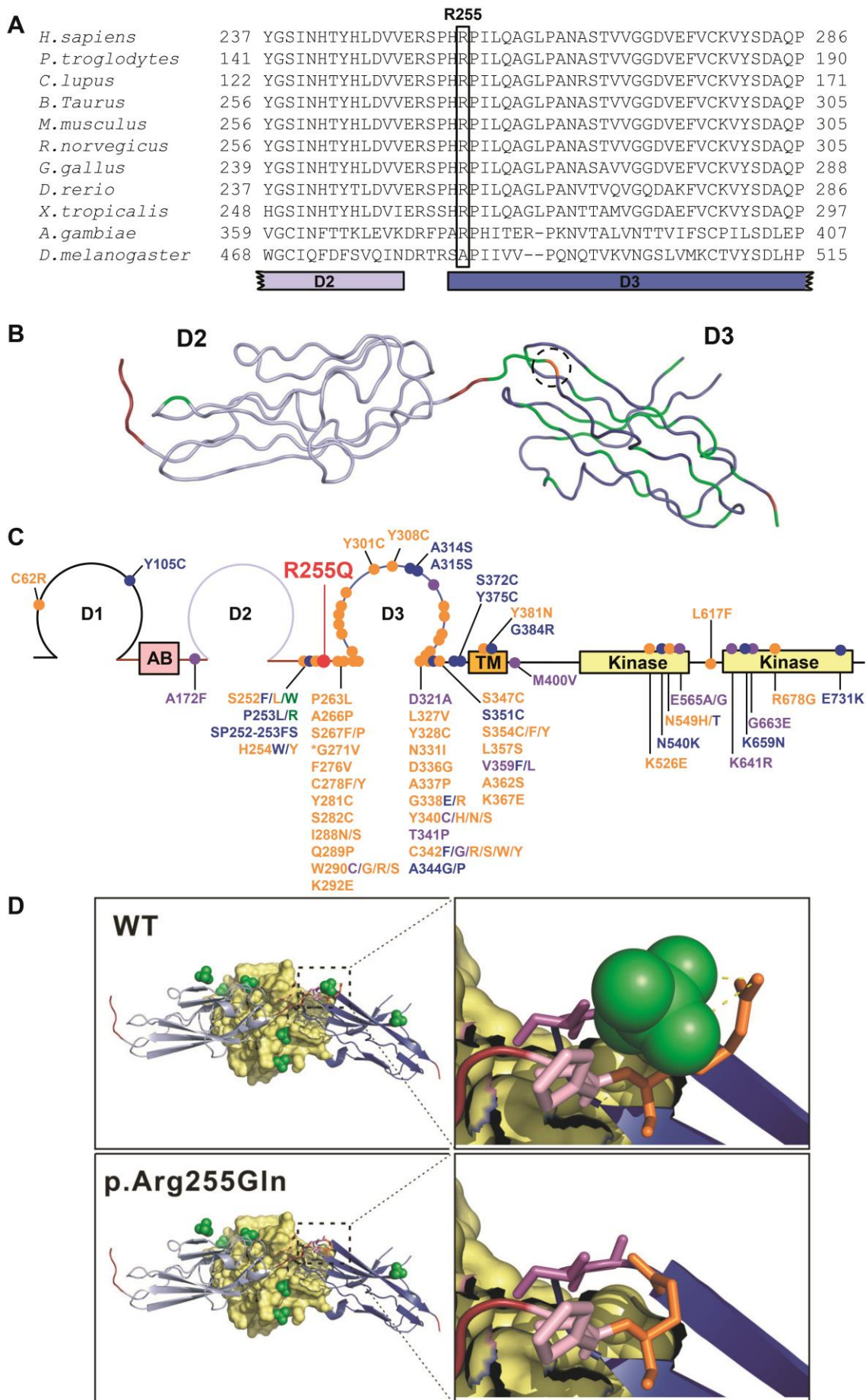


Figure 5. FGFR2 and ERK1/2 activation studies to determine effect of p.R255Q on FGFR2 function. HEK293 cells were transfected with FGFR2 WT or mutant constructs. After 20 h, the cells were serum starved for 4 h and then 20 ng/ml FGF2 with 10 μ g/ml heparin was added. **A:** Cells were harvested after 0, 5 and 15 min, lysates run on western blots, and blots probed with anti-phospho ERK1/2, anti-ERK1/2, anti-phospho-tyrosine and anti-FGFR2 antibodies. **B:** Bar graph showing the densitometric quantification of FGFR2 phosphorylation levels from a representative western blot. **C:** ERK1/2 phosphorylation levels were quantified and standardized to unphosphorylated protein. Protein band intensities across blots were normalized to the standardized p-ERK value for FGFR2 WT at time 0 (set to 1). The graph shows the mean \pm S.E.M. of 4 independent experiments. Statistical analysis was performed using Mann-Whitney test.

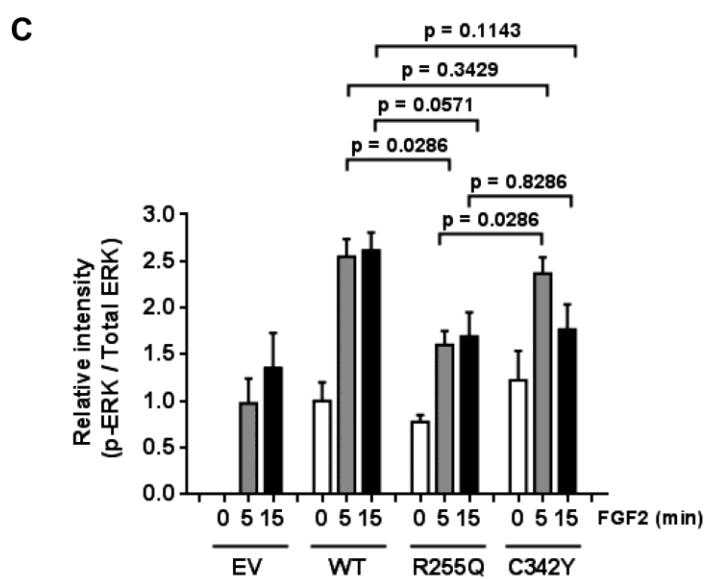
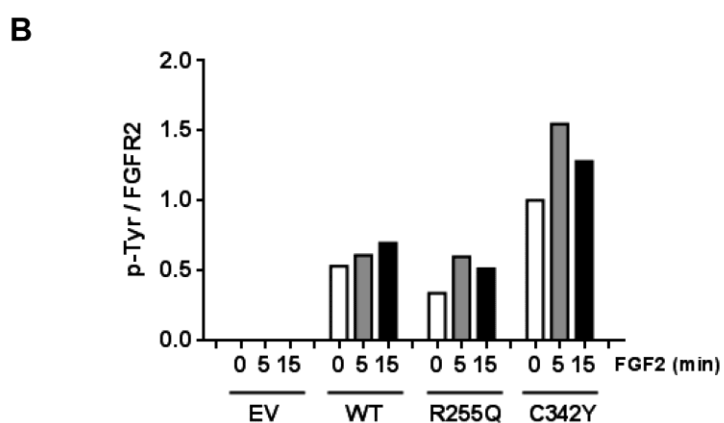
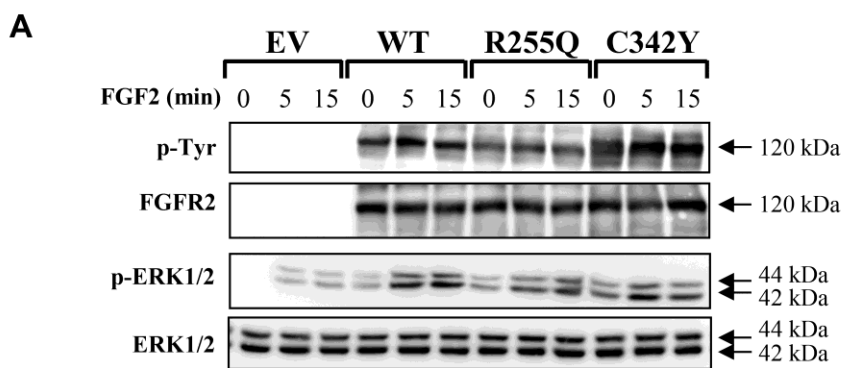


Table 1. Germline gene mutation candidates identified by whole exome sequencing.

Gene (OMIM)	Genomic Variant	cDNA Variant	Protein Variant	GERP	PolyPhen2 Prediction	CADD (v1.3)	ExAC (Alt/Ref)	Disease (OMIM ID) (inheritance)	Exclusion Criteria
<i>FGFR2</i> (176943)	chr10:g. 123,279,668 C>T	c.764G>A <i>NM_000141.4</i>	R255Q NP_000132.3	5.79	Probably damaging	35	Novel (0/110,500)	Crouzon syndrome (CFD1; 123500) (AD) Apert syndrome (ACS1; 101200) (AD) Pfeiffer syndrome (ACS5; 101600) (AD) Jackson-Weiss syndrome (JWS; 123150) (AD)	None (N.B. not AD inheritance gain- of-function mutation like all currently reported mutations in OMIM)
<i>UBE2Q2</i> (612501)	chr15:g. 76,168,613_ 76,168,614 dupGT	c.673+1_+2 dupGT <i>NM_173469.3</i>	*Splice site (donor)	5.00	No prediction	26	Novel (0/121,300)	None	Expressed in all tissues.
<i>COL12A1</i> (120320)	chr6:g. 75,843,078 A>G	c.5725T>C <i>NM_004370.5</i>	Y1909H NP_004361.3	5.63	Probably damaging	23.3	Novel (0/120,634)	Bethlem myopathy (BTHLM2; 616471) (AD) Ullrich congenital muscular dystrophy-2 (UCMD2; 616470) (AR)	Patient showed no evidence of contractures. Bethlem Myopathy does not cause limb abnormalities or acinar dysplasia. Muscle histology was normal at autopsy.
<i>GGA3</i> (606006)	chr17:g. 73,235,102 T>C	c.1744A>G <i>NM_014001.4</i>	K582E NP_054720.1	5.24	Possibly damaging	24.8	Novel (0/121,114)	None	Expression in lung but not limbs

Variants were identified by whole exome sequencing. These 4 candidate variants are changes in highly conserved amino acids, are in conserved regions across species, and are predicted to negatively impact protein function. Asterisk, *UBE2Q2* (dupGT) is predicted by splice predictor programs Alternative Splice Site Predictor and Alamut 2.0 Splicing Prediction Module to potentially cause a 2 nt frameshift. Autosomal dominant, AD; Autosomal recessive, AR. Expression was determined using BioGPS, MGI and GenePaint. For cDNA numbering, nucleotide numbering uses +1 as the A of the ATG translation initiation codon in the reference sequence, with the initiation codon as codon 1.